

# Seawater Distillation with $\text{Be}_3\text{C}_2$ Monolayer: Case Study by DFT

## Abstract

The predicted structure of the  $\text{Be}_3\text{C}_2$  monolayer has been investigated using ab-initio calculations and density functional theory, for which the full potential linear augmented plane waves plus local orbital (FP-LAPW+Lo) and the Perdew–Burke–Ernzerhof generalized gradient approximation (PBE-GGA) functional methods have been used. This structure has a uniform porosity and its pore size is 5.7 Å, which is very suitable for water nanofiltration. After studying the electronic properties of the  $\text{Be}_3\text{C}_2$  monolayer to use it as nanofiltration, one and two molecular clusters of water are adsorbed on it. The adsorption energy and the penetration of water molecules in the  $\text{Be}_3\text{C}_2$  monolayer are investigated. There is a discussion about its encouraging prospective application in highly efficient nanofiltration membranes for the desalination of seawater.

**Keywords:** Nanofiltration, Membrane, Desalination, Monolayer, Barrier energy, DFT

**Roya Bakhshkandi<sup>1</sup>,  
Mohammad  
Samipoorgiri<sup>\*2</sup>, Mansour  
Rezaei Mersagh<sup>3</sup>,  
Mostafa Sefidgar<sup>4</sup>**

<sup>1</sup>Department of Physics, Islamic Azad University, North Tehran Branch, Tehran, Iran.

<sup>2</sup>Department of Chemical Engineering, Islamic Azad University, North Tehran Branch, Tehran, Iran.

<sup>3</sup>Department of Physics, Islamic Azad University, North Tehran Branch, Tehran, Iran

<sup>4</sup>Department of Mechanical Engineering, Islamic Azad University, Pardis Branch, Tehran, Iran

\*\*Correspondence author:

Email: [M\\_samipoor@iau-tnb.ac.ir](mailto:M_samipoor@iau-tnb.ac.ir)

## Introduction

### 1. Introduction

About one-third of the world's population is currently facing water shortages, which is projected to increase to two-thirds of the world's population by 2030 [1]. Therefore, freshwater resources are very scarce and access to them is rapidly declining due to population growth, agriculture, industrial expansion, and climate change, etc., indicating a kind of global crisis [2]. Hence, desalination is a promising method for providing safe water from the waters of seas and oceans, which make up 97% of the total water of the earth [3]. Desalination provides a good hydrological cycle for producing safe water from oceans and seas. There are different industrial solutions and methods for desalination requiring high initial and current costs and high energy consumption, which is one of the challenges facing the 21st century [4].

The first step is to direct desalination to methods with the least energy consumption and current and initial costs [5]. Thus, in order to achieve these goals, the first step is to change the membrane technology as the most widely used method. The development of nanotechnology has made it possible to make new membranes, the most important feature of which is the need for less energy for desalination [6]. The unique structural and morphological properties of nanomaterials for use in saline water treatment and desalination have attracted considerable attention. The result of recent advances in this field can be seen in membranes with high water flux and excellent salt repellency [7]. However, the economic feasibility of these nanomaterials remains questionable [8].

Membrane separation technology has advantages such as lower energy consumption and lower investment costs than conventional separation methods, and in addition to the simplicity of the process, it requires less equipment [9]. Many studies have shown that the reverse osmosis method consumes less energy than other methods [10]. Desalination plants typically have a widespread negative impact on the surrounding ecosystem and environment [11].

Over the past few decades, the use of membranes has expanded significantly, and they are now used in a wide variety of industries to separate gas and liquid [12,13]. This wide range of applications is due to their usefulness and special features such as their small size for large surface membrane areas, compactness, ease of fabrication, operation, and design of prefabricated samples [14,15].

With the advent of one-dimensional and two-dimensional carbon nanomaterials, the membranes studied today are made of graphene or carbon nanotubes. To achieve desalination membranes, nanometer porosity is created on single-layer or multi-layer graphene surfaces by various methods such as ion bombardment. These pores are then chemically functionalized to physically prevent the passage of water-soluble ions [16]. The desalination capacity of this type of membrane strongly depends on the diameter of the pores created on the graphene surface or the diameter of the carbon nanotubes [17-20]. In this study, a  $\text{Be}_3\text{C}_2$  monolayer membrane is also examined with a suitable pore size for water distillation, which is organized as follows: In Section 2, there are details of the calculations and the simulation method. In Section 3, the structural and electronic properties of the  $\text{Be}_3\text{C}_2$  monolayer are examined. In

Section 4, as an exploratory study, the influence of the use of  $\text{Be}_3\text{C}_2$  monolayer as nanofiltration is investigated by the adsorption of water molecules, and finally, the results are summarized [15,12-14].

## 2. Computational Details

The Density Functional Theory framework and full potential linear augmented plane waves plus local orbital (FP-LAPW+lo) methods [21] are used to perform the calculations as well as the Perdew–Burke–Ernzerhof generalized gradient approximation (PBE-GGA) [22,23] which are used by WIEN2k package [24]. The input parameters are optimized to  $R_{\text{Kmax}}=8.0$ ,  $G_{\text{max}}=14.0$ , and  $K\text{-Point}=4000$ . Owing to symmetry, the five positions of the selected space group,  $p6/mmm(191)$ , are reduced to two positions. The obtained lattice constants are  $a=b=5.68 \text{ \AA}$  and  $c=10 \text{ \AA}$ . The mini position command is utilized to relax the structure with  $1.0 \text{ a.u./dyne}$  accuracy [25]. Except for Figure 1, which is depicted by the XcrysDen package [26], all other figures are depicted by SigmaPlot software.

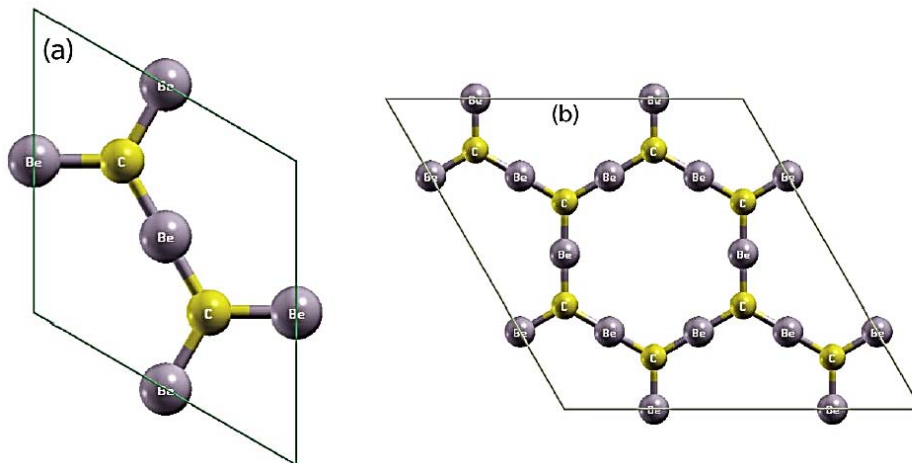
## 3. Structural and Electronic Properties

The  $\text{Be}_3\text{C}_2$  structure was predicted in 2017 by Bing Wang et al. This structure is a hexagonal monolayer structure which is similar to the T-Carbon graphene-like monolayer structure [27]. In the equilibrium state, two C atoms and three Be atoms are in the structure of its unit cell, which is shown in Figure 1a. Be atoms in Wyckoff locations are bridges between two C

atoms with which they form strong  $\sigma$  bonds. Figure 2(b) also illustrates a  $2\times 2\times 1$  supercell of this structure. The bond length of Be-C is  $1.64 \text{ \AA}$ , and the bond angle is  $120$  degrees.

For the stability of this structure and according to the reference [28], the formation energy is calculated chemically, the value of which is equal to  $-0.99 \text{ eV/atom}$ . Moreover, for dynamic stability, phonon calculations are obtained, and no imaginary negative mode has been observed. Another emphasis on the stability of this system is its thermal stability calculations, demonstrating that this structure maintains its original configuration up to  $900 \text{ K}$ .

To reveal the mechanical stability of a system, the energy-volume diagram (E-V) (Figure 1), another tool of computational physics, requires a minimum as proof of stability, and acceptable lattice constants can be obtained by fitting the Birch-Murnaghan equation with the E-V diagram;  $a=b=5.69 \text{ \AA}$  and  $c=10 \text{ \AA}$ .



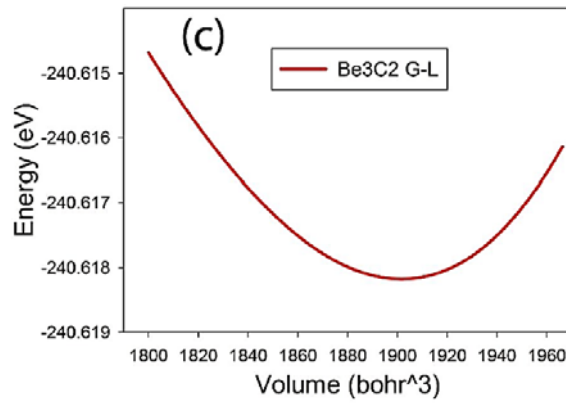


Figure 1. Top views of the (a) unit cell and (b)  $2 \times 2 \times 1$  supercell structure and (c) energy–volume ( $E$ – $V$ ) curve of  $\text{Be}_3\text{C}_2$ .

In this section, the electronic properties of the  $\text{Be}_3\text{C}_2$  monolayer are examined and compared with the results obtained in reference [28]. To evaluate its electronic properties, band structure and total and partial density of states diagrams are shown in Figure 2. As shown in Figure 2a, the two bands of VBM and CBM touch each other at the Fermi level at the Dirac  $k$  point, indicating the zero energy gap semiconductor properties for this structure, and it is the so-called Dirac cone which is observed and confirmed in the DOS diagram in Figure 2b. It is clear from Figure 2 (b) that the Dirac

state near the Fermi level is composed of the hybridization of the  $p$  orbitals of the Be and C atoms. In this structure, a strong  $\sigma$  bond is established between the Be and C atoms, and each C atom is hybridized by  $sp^2$  to three Be atoms as a triangular, as shown in Figure 2 (b). In this figure, the  $p_z$  orbital for the two atoms of Be and C has the largest share in VBM and CBM to form the Dirac cone, and the share of the  $s$ ,  $p_x$ , and  $p_y$  orbitals of these two atoms is negligible. It is noteworthy that these calculations are in good agreement with the reference [28].

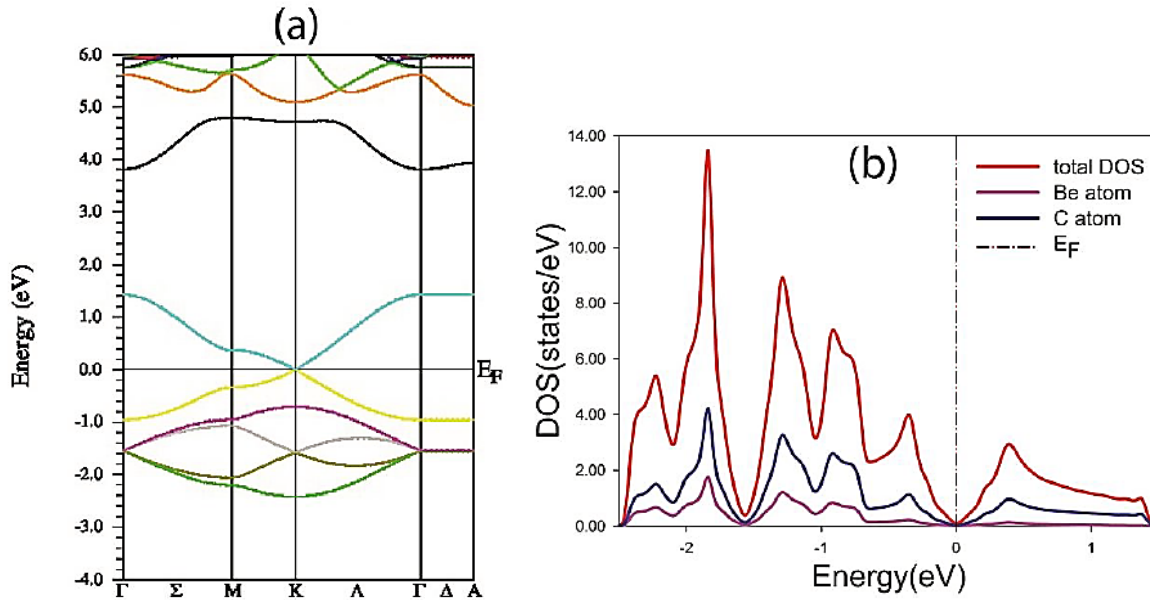


Figure 2. (a) Band structure and (b) DOS diagrams of  $\text{Be}_3\text{C}_2$  monolayer.

## 4. Result and Discussion

### 4.1. Water Nanofiltration

Figure 1b illustrates a  $2 \times 2 \times 1$  supercell of the  $\text{Be}_3\text{C}_2$  monolayer structure. In a hexagonal pore, the distance between two atoms facing each other is  $6.57 \text{ \AA}$  and the distance between two facing Be atoms is  $5.69 \text{ \AA}$ , with the atoms measured center-to-center. Experimental studies reveal that the size of the graphene pore in the optimized state must be  $0.4 \pm 0.24 \text{ nm}$  in size to allow a

molecule of water to pass through and also to reject inorganic salt ions [15, 29]. It should be noted, however, that the Van der Waals diameter of a molecule of water is  $0.275 \text{ nm}$  [30]. In addition, hydrated salt ions are often about  $0.7 \text{ nm}$  in diameter or even larger, for example,  $\text{Na}^+ = 0.72 \text{ nm}$ ,  $\text{K}^+ = 0.67 \text{ nm}$ , and  $\text{Cl}^- = 0.66 \text{ nm}$  [31,32].

Two-dimensional materials are very attractive for ionic and molecular nanofiltration, but they are limited in wide areas by

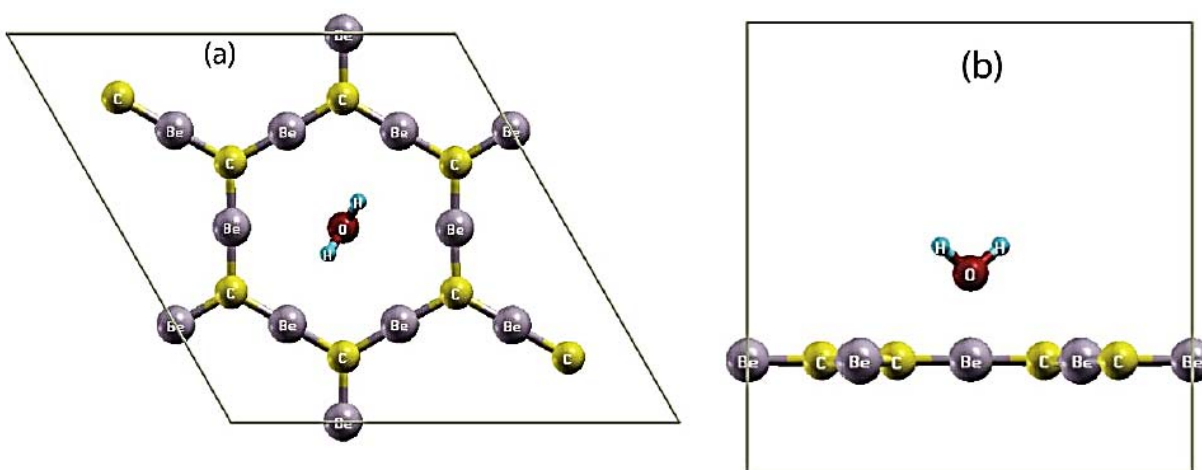
extended mechanical resistance. In 2019, Yanbing Yang et al experimentally used a GNM/SWNT composite membrane to desalinate water. Using this structure, they showed high water permeability as well as a high rate of rejection of salt ions or organic molecules. In their structure, most of the pores in the hybrid membrane were obtained between  $4\text{Å}$  and  $7\text{Å}$  [33]. According to the above and the values obtained from the  $\text{Be}_3\text{C}_2$  monolayer structure located in Figure 1b, the pore size in the  $\text{Be}_3\text{C}_2$  monolayer corresponds very well with the optimized size for water nanofiltration. For high permeability, a solvent requires a membrane as thin as possible [34,35], with the  $\text{Be}_3\text{C}_2$  monolayer structure possessing these characteristics. Therefore, the  $\text{Be}_3\text{C}_2$  monolayer has excellent properties as a single membrane for the desalination of water. The pore size as a physical sieve determines the rejection of organic dyes and ion salts.

#### 4.2. Water Absorption on $\text{Be}_3\text{C}_2$ Monolayer

In this section, the interaction between the water molecules and the  $\text{Be}_3\text{C}_2$  monolayer surface is investigated as water permeability on the  $\text{Be}_3\text{C}_2$  monolayer. First, a water molecule is placed on a  $2\times 2\times 1$  supercell structure with a pore approximately  $5.70\text{Å}$  in diameter shown in Figure 1b. After relaxing the structure, it was found that the most stable place for the adsorption of an  $\text{H}_2\text{O}$  molecule on the  $\text{Be}_3\text{C}_2$  monolayer is its hexagonal center, which is illustrated in Figure 4 (a) and

(b) in both the top and side views. Moreover, after relaxing the structure of the water molecule, it was placed at a distance of  $1.95\text{Å}$  from its hexagonal center, which is the distance of the O atom to the center of the hexagonal pore, and the two H atoms are placed aligned in with each other with two opposite Be atoms. The distance from the H atom to its nearest neighbor is  $3.29\text{Å}$ , which is longer than the range of Be-H hydrogen bonds. Hence, there is no chemical bond between the water molecule and the neighboring atoms, and it is more of a weak van der Waals type. As shown in Figure 3 (ab), the  $\text{H}_2\text{O}$  molecule is perpendicular to the  $\text{Be}_3\text{C}_2$  surface, and the distance of the O atom with the neighboring carbon atoms is  $3.80\text{Å}$  and with the Be atoms, which are aligned with the H direction of the water molecule, is  $3.44\text{Å}$  with 4 atoms as well as  $3.41\text{Å}$  with the other four Be atoms. It can be concluded that because of the adsorption of a single molecule of  $\text{H}_2\text{O}$ , the Be atoms have slightly shifted from their two-dimensional plane, so the  $\text{Be}_3\text{C}_2$  monolayer has a slight curvature.

In terms of electronic properties, the structure under the influence of this water molecule has a wider energy gap to turn into a semiconductor with an energy gap of  $0.37\text{eV}$ , the DOS diagram of which is depicted in Figure 3c.



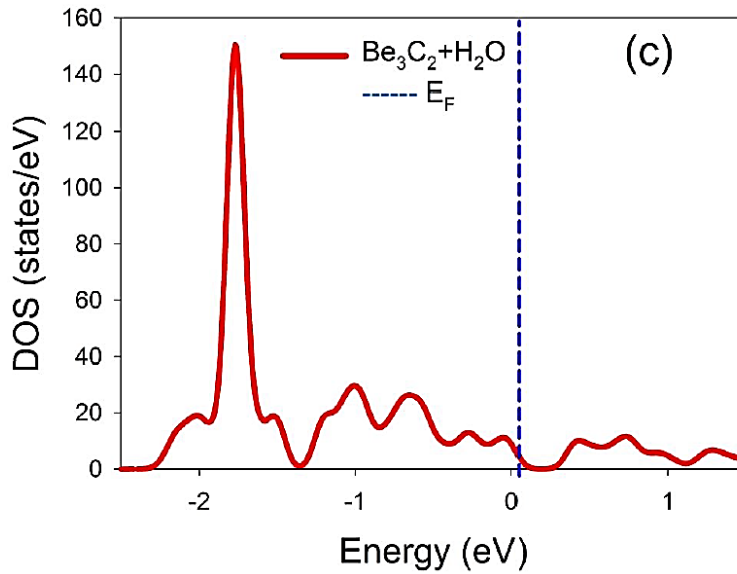


Figure 3. (a), (b) top and side view for single H<sub>2</sub>O adsorption on Be<sub>3</sub>C<sub>2</sub> monolayer and (c) total DOS for this case.

The adsorption energy can reflect the strength of the interaction between the Be<sub>3</sub>C<sub>2</sub> monolayer and the water molecules, so it is calculated for this purpose. In this structure, the adsorption energy is obtained from the following equation:

$$E_{ads} = \frac{1}{n} [E_{tot} - (nE_{H_2O} + E_{Be_3C_2})] \quad (1)$$

In this equation,  $E_{ads}$  is adsorption energy,  $E_{tot}$  is equal to the energy of the whole system on which water molecules are absorbed,  $E_{H_2O}$  is the total energy of an isolated water molecule,  $E_{Be_3C_2}$  is the energy of Be<sub>3</sub>C<sub>2</sub> monolayer, and  $n$  is the number of water atoms. The calculated amount of adsorption energy is about 0.042 eV, indicating that there is no chemical bond between the H<sub>2</sub>O molecule and the Be<sub>3</sub>C<sub>2</sub> monolayer, which is slightly larger than the adsorption of a water molecule on graphene (0.03 eV) [36] and less than T-C<sub>3</sub>N (0.617 eV) [27]. This adsorption energy demonstrates that there is no

chemical bond between the water molecule and the Be<sub>3</sub>C<sub>2</sub> monolayer, and the bond is of the physically weak Van der Waals type. The adsorption of a water molecule on the Be<sub>3</sub>C<sub>2</sub> monolayer is an exothermic process.

In Figure 4, the energy profile is calculated, expressing the state of water penetration in the shortest passage path, which is obtained with an energy barrier of 23.03 kcal/mol. As it is known, reactions equal to or less than 21 kcal/mol can easily continue at room temperature [37]. Nevertheless, this barrier is obtained from the DFT calculation in which only one water molecule is considered, without any environmental effects as well as pressure and temperature conditions. Osmotic pressure applied to one side of the Be<sub>3</sub>C<sub>2</sub> monolayer and other environmental factors can help water molecules easily pass through this barrier.

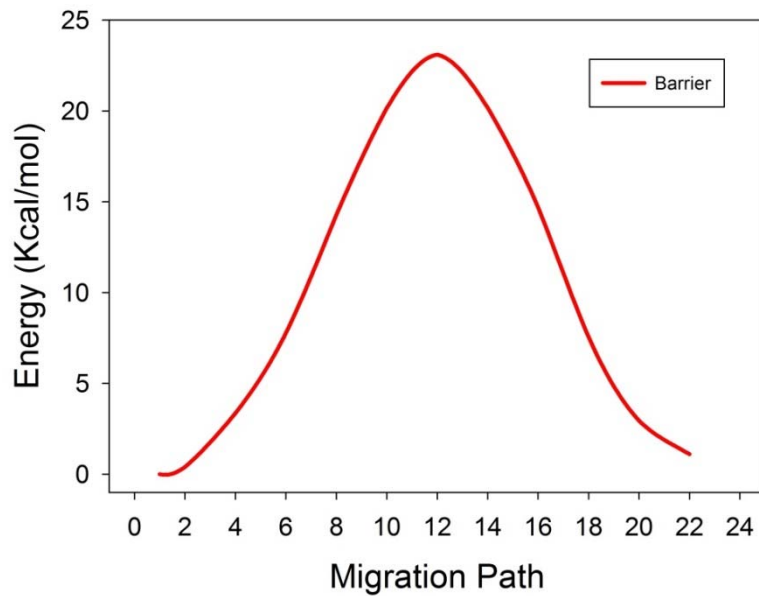


Figure 4. Energy profile one water molecule penetrating along the minimum migration path through a pore on Be<sub>3</sub>C<sub>2</sub> monolayer

Such a calculated geometric arrangement for small blue clusters is in good agreement with previously reported papers [27, 38, 39].

## 5. Conclusion

The structural and electronic properties of this material are investigated by the computational method to be consistent with the previous work done on the Be<sub>3</sub>C<sub>2</sub> structure. It is a structure similar to a graphene-like T-carbon monolayer, which is electronically a semiconductor with zero electronic gaps and is one of the Dirac cone nanomaterials. Due to the very suitable pore size (5.7 Å) in the Be<sub>3</sub>C<sub>2</sub> monolayer, water adsorption on this material has been studied. The calculations demonstrate that this pore size rejects mineral salt ions and organic pollutants in water, so that water molecules pass, leading to water desalination. The adsorption energy of one H<sub>2</sub>O molecule on the Be<sub>3</sub>C<sub>2</sub> monolayer has adsorption energy of 0.042 eV, creating no chemical bond between the water molecule and the structure, allowing water molecules to pass easily through the structure pores. However, there is a weak van der Waals physical bond between the water molecule and the Be<sub>3</sub>C<sub>2</sub> monolayer. The energy barrier value for the shortest possible path of this structure is calculated to be 23.03 kcal/mol, which, considering the computational constraints and environmental conditions, water molecules can overcome and cross this energy barrier even at room temperature. Appropriate pore size, high density of pores and their uniform distribution on the surface, very thin thickness, type of bond, and unique mechanical properties of this structure are so convincing that this material has a promising potential application in seawater desalination and water treatment. The authors declare that they have no conflict of interest.

## Funding:

This research received no specific grant from any funding agency in the public, commercial, or not-for-profit sectors.

## Ethical statements:

Hereby, M.Samipoorgiri consciously assure that for the manuscript "Seawater Distillation with Be<sub>3</sub>C<sub>2</sub> Monolayer: Case Study by DFT" the following is fulfilled:

- 1) This material is the authors' own original work, which has not been previously published elsewhere.
- 2) The paper is not currently being considered for publication elsewhere.
- 3) The paper reflects the author's own research and analysis in a truthful and complete manner.
- 4) The paper properly credits the meaningful contributions of co-authors and co-researchers.
- 5) The results are appropriately placed in the context of prior and existing research.
- 6) All sources used are properly disclosed.
- 7) All authors have been personally and actively involved in substantial work leading to the paper and will take public responsibility for its content.

## Reference

- [1] Virakul B.,2015, Global challenges, sustainable development, and their implications for organizational performance. *European Business Review*. Jun 8,DOI: /10.1108/EBR-02-2014-0018/full/html.
- [2] Koop, S.H.A.Van Leeuwen,C.J.2017, The challenges of water, waste and climate change in cities, *Environment, Development and Sustainability*, vol.19, pp. 85–418, DOI: /10.1007/s10668-016-9760-4.
- [3] Sunagawa,S., Acinas,S,G., Bork, P., Bowler, C., et all,2020, Tara Oceans: towards global ocean ecosystems biology, *nature reviews microbiology*, vol.18, pp. 428–445, DOI: /10.1038/s41579-020-0364-5.

- [4] Boretti, A., Rosa, L., 2019, Reassessing the projections of the World Water Development Report, npj nature partner journals, vol.2, no.15, DOI: /10.1038/s41545-019-0039-9.
- [5] Goh, P.S., Lau, 2018, W.J., Othman, M.H.D., Ismail, A.F. Membrane fouling in desalination and its mitigation strategies, *Desalination*, vol.425, pp.130–155, DOI: /10.1016/j.desal.2017.10.018.
- [6] Nunes, S.P., Culfaz-Emecen, Z.P., Ramon, G.Z., Visser, t., Koops, G.H., Jin, W., Ulbricht, M., 2020, Thinking the future of membranes: Perspectives for advanced and new membrane materials and manufacturing processes, *MembraneScience*, vol.598, pp.117761, DOI: /10.1016/j.memsci.2019.117761.
- [7] Ray. S.S., Bakshi, H.S., Dangayach, R., Singh, R., Kanti Deb, C., Ganesapillai, M., Chen, S., Purkait, M.K., 2020, Recent Developments in Nanomaterials-Modified Membranes for Improved Membrane Distillation Performance, *Membranes (MDPI)*, vol.10(7), pp.140, DOI: 10.3390/membranes10070140.
- [8] Daer, S., Kharraz, J., Giwa, A., Wajih Hasan., S., 2015, Recent applications of nanomaterials in water desalination: A critical review and future opportunities, *Desalination*, vol.367, pp.37-48, DOI: /10.1016/j.desal.2015.03.030.
- [9] Souari, L., Hassairi, M., 2007, seawater desalination by reverse osmosis: the true needs for energy, *Desalination*, no. 206, pp. 465–473, DOI: 10.1016/j.desal.2006.02.073.
- [10] Schunke, A.J., Herrera, G.A., H. Padhye, L., Berry, T. A., 2020, Energy Recovery in SWRO Desalination: Current Status and New Possibilities, *VOL.9*, pp.1-4, DOI: 10.3389/frsc.2020.00009.
- [11] Areiqat, A., Mohamed, K.A., 2005, Optimization of the negative impact of power and desalination plants on the ecosystem, *J.Desalination*, vol.185, pp.95-103. <https://doi.org/10.1016/j.desal.2005.04.038>.
- [12] Nogalska, A., Trojanowska, A., Garcia-Valls, R., 2017, Membrane contactors for CO<sub>2</sub> capture processes – a critical review, *Physical Sciences Reviews*, vol.2, pp.5, DOI: 10.1515/psr-2017-0059.
- [13] Adham, S., Hussain, A., Minier-Matar, J., Janson, A., Sharma, R., 2018, Membrane applications and opportunities for water management in the oil & gas industry, *Desalination*, vol.440, pp.5-6, DOI: 10.1016/j.desal.2018.01.030.
- [14] Jordan, J., Jacob, K.I., Tannenbaum, R., Sharaf, M.A., Jasiuk, I., 2005., Experimental trends in polymer nanocomposites—a review, *Materials Science and Engineering A*, 393-1-11, DOI: 10.1016/j.msea.2004.09.044.
- [15] Mahmoud, K. A., Mansoor, B., Mansour, A., Khraisheh, M., 2015, Functional graphene nanosheets: the next generation membranes for water desalination, *Desalination*, vol. 356, pp.208-225, DOI: 10.1016/j.desal.2014.10.022.
- [16] Homaeigohar, S., Elbahri, M., 2017, Graphene membranes for water desalination, *NPG Asia Materials*, vol.427, pp.2-4, DOI: 10.1038/am.2017.135.
- [17] Aende, A., Gardy, J., Hassanpour, A., 2020, Seawater Desalination: Review of Forward Osmosis Technique, Its Challenges, and Future Prospects, *Processes MDPI*, 8(8), 901, DOI: [org/10.3390/pr8080901](https://doi.org/10.3390/pr8080901).
- [18] Mahmoud. K.A., Mansoor, B., Mansour, A., Khraisheh, M., 2015, Functional graphene nanosheets: The next generation membranes for water desalination, *Desalination*, vol. 367 pp.208-225, DOI: /10.1016/j.desal.2014.10.022.
- [19] Aghigh, A., Alizadeh, V., Wong, H.Y., Islam, M.S., Amin, N. and Zaman, M., 2015. Recent advances in utilization of graphene for filtration and desalination of water: A review. *Desalination*, 365, pp.389-397, DOI: 10.1016/j.desal.2015.03.030.
- [20] Liu, G., Wanqin, J., Nanping X., 2015, Graphene-based membranes, *Chemical Society Reviews*, vol.44, pp.5016-5030, DOI: 10.1039/c4cs00423j.
- [21] Georg, K. H. Madsen, G.K.H., Blaha, P., Schwarz, K., Sjöstedt, E., Nordström, L., 2001, Efficient linearization of the augmented plane-wave method, *Phys. Rev. B*, vol.64, 195134, DOI: 10.1103/PhysRevB.64.195134.
- [22] Blaha, P., Schwarz, K., Madsen, G. K.H., Kvasnicka, D., Luitz, J., et al., 2021, WIEN2K, An Augmented Plane Wave Plus Local Orbitals Program for Calculating Crystal Properties, Vienna University of Technology, Vienna, Austria, <https://repositum.tuwien.at/handle/20.500.12708/100909?mode=full>.
- [23] Perdew, J.P., Chevary, J.A., Vosko, S. H., Jackson, K. A., Pederson, M. R., Singh, D. J., Fiolhais, C., 1992, Atoms, molecules, solids, and surfaces: Applications of the generalized gradient approximation for exchange and correlation, *Phys. Rev. B*, vol.46, 6671, DOI: 10.1103/PhysRevB.46.6671.
- [24] Blaha, P., Schwarz, K., Sorantin, P., Trickey, S. B., 1990, Full-potential, linearized augmented wave programs for crystalline systems, *computer Phys. Commun*, vol.59, pp.399–415, DOI: 10.1016/0010-4655(90)90187-6
- [25] Kronig, R.L., 1926, On the Theory of Dispersion of X-Rays, *J. Opt. Soc. Am*, vol.12, pp.547-557, DOI: 10.1364/JOSA.12.000547.
- [26] Kokalj, A., 2003, Computer graphics and graphical user interfaces as tools in simulations of matter at the atomic scale, *Comput.Mater. Sci*, vol.28, pp.155–168, DOI: 10.1016/S09270256(03)00104-6.
- [27] Zhou, J., Li, L., Fu, C., Wang, J., Fu, P., Kong, C., Bai, F., Eglitis, R. I., Zhang, H., Jia, R., 2020, A novel T-C3N and seawater desalination, *Nanoscal.*, DOI: 10.1039/C9NR08108A.
- [28] Wang, B., Yuan, S., Li, Y., Shi, L., Wang, J., 2017, A New Dirac Cone Material: A Graphene-like Be<sub>3</sub>C<sub>2</sub> Monolayer, *Nanoscale*, vol, 9, pp. 5577–5582, DOI: 10.1039/c7nr00455a.
- [29] O'Hern, S. C., Boutilier, M. S., Idrobo, J. C., Song, Y., Kong, J., Laoui, T., Atieh, M., Karnik, R., 2014, Selective ionic transport through tunable subnanometer pores in single-layer graphene membranes, *Nano Lett.*, vol.14, pp.1234-1241, DOI: [abs/10.1021/nl404118f](https://doi.org/abs/10.1021/nl404118f).
- [30] Cohen-Tanugi, D., Grossman, J. C., 2012, Water desalination across nanoporous graphene, *Nano Lett.* vol.12, 3602C3608, DOI: 10.1021/nl3012853. 13
- [31] Cohen-Tanugi, D., Grossman, J. C., 2015, Nanoporous graphene as a reverse osmosis membrane: recent insights from theory and simulation, *Desalination*, vol. 366, 59C70, DOI: 10.1016/j.desal.2014.12.046.
- [32] Xu, K., Feng, B., Zhou, C., Huang, A., 2016, Synthesis of highly stable graphene oxide membranes on polydopamine functionalized supports for seawater desalination, *Chem. Eng. Sci.* ,vol.146, pp. 159-165, DOI: 10.1016/j.ces.2016.03.003.
- [33] Yang, Y., Yang, X., Liang, L., Gao, Y., Cheng, H., Li, X., Zou, M., Cao, A, Ma, R., Yuan, Q., Duan, X., 2019, Large-area graphene-nanomesh/carbon nanotube hybrid membranes for ionic and molecular nanofiltration, *Science*, vol.364, pp.1057-1062, DOI: [abs/10.1126/science.aau5321](https://doi.org/abs/10.1126/science.aau5321).
- [34] Karan, S., Samitsu, S., Peng, X., Kurashima, K., Ichinose, I., 2012, Ultrafast Viscous Permeation of Organic Solvents Through Diamond-Like Carbon Nanosheets, *Science*, vol, 335, pp.444, DOI: [abs/10.1126/science.1212101](https://doi.org/abs/10.1126/science.1212101).
- [35] Nair, R. R., Wu, H. A., Jayaram, P. N., Grigorieva, I. V., Geim, A. K., 2012, Unimpeded Permeation of Water Through Helium-Leak-Tight Graphene-Based Membranes, *Science*, vol, 335, pp. 442, DOI: [abs/10.1126/science.1211694](https://doi.org/abs/10.1126/science.1211694).
- [36] Fu, P., Jia, R., Kong, C.-P., Eglitis, R. I., Zhang, H.-X., 2015, From the determination of the fugacity coefficients to the estimation of hydrogen storage capacity: A convenient theoretical method, *Hydrogen Energy*, vol.40, pp.10908- 10917, DOI: 10.1016/j.ijhydene.2015.07.005.
- [37] Young, D. C., 1997, *Computational Chemistry: A Practical Guide for Applying Techniques to Real-World Problems*, pp. 147, Wiley-Interscience, John Wiley & Sons, Inc., Publication, <https://www.wiley.com/enus/Computational+Chemistry:+A+Practical+Guide+for+Applying+Techniques+to+Real+World+Problems-p-9780471333685>.
- [38] Maheshwary, S., Patel, Sathyamurthy, N., Kulkarni, A. D., Gadre, S. R., 2001, Structure and stability of water clusters (H<sub>2</sub>O)<sub>n</sub>, n = 8-20: An ab initio investigation, *J. Phys. Chem. A*, vol. 105, pp.10525-10537, DOI: 10.1021/jp013141b.
- [39] Lehmann, S. B. C., Spickermann, C., Kirchner, B., 2009, Quantum Cluster Equilibrium Theory Applied in Hydrogen Bond Number Studies of Water. I. Assessment of the Quantum Cluster Equilibrium Model for Liquid Water, *J. Chem. Theory Comput.*, vol.5, pp.1640-1649, DOI: 10.1021/ct800310a.